Citation: Jian-Xin Lu, Bao-Jian Zhan, Zhen-Hua Duan, Chi Sun Poon, Using glass powder to improve the durability of architectural mortar prepared with glass aggregates, Materials and Design 135 (2017) 102–111. http://dx.doi.org/10.1016/j.matdes.2017.09.016

Using glass powder to improve the durability of architectural mortar prepared with glass aggregates

Jian-Xin Lu [a], Bao-Jian Zhan [a], Zhen-Hua Duan [a,b], Chi Sun Poon [a,*]

[a] Department of Civil and Environmental Engineering, The Hong Kong Polytechnic University, Hung Hom, Kowloon, Hong Kong

[b] Department of Structural Engineering, Tongji University, Shanghai, People's Republic of China

Corresponding author: cecspoon@polyu.edu.hk

Abstract:

This study designed a novel cement-based architectural tile prepared with more than 70% waste glass content (by weight). The waste glass was employed not only as decorative aggregates but also as a supplementary cementitious material in the architectural mortar. In terms of shrinkage, the incorporation of glass powder (GP) could significantly reduce the drying shrinkage of the glass mortars regardless of its fineness. When the glass mortars were subjected to high temperature (800 °C), the inclusion of GP into the mortars was more able to mitigate the flexural and compressive strengths losses as compared to the control glass mortar prepared without the use of GP. Furthermore, using the GP and glass aggregates simultaneously could effectively improve the resistance of the glass mortars to sulfuric acid attack and the positive effect was more pronounced when finer GP was incorporated. In particular, an encouraging result shows that the replacement of 20% cement by fine GP successfully suppressed the deteriorative alkali-silica-reaction (ASR) expansion caused by the glass aggregates. Also, the glass mortars incorporated with fine GP exhibited comparable or even superior durability properties than that of the fly ash blended glass mortar.

Keywords: Glass powder; Glass aggregates; Durability; Architectural mortar

1 Introduction

Due to the excellent characteristics of glass, such as optical transparency, chemical inertness, high intrinsic strength and low gas permeability [1], glass container is the most commonly used form of packaging beverage material. The most common type of beverage glass containers used is soda-lime-silica glass, which usually contains 10~20 mol% Na_2O, 5~15 mol% CaO and 70~75 mol% SiO_2 [2]. Data from the Environmental

Protection Department (EPD) indicated that, in Hong Kong, 275 tones waste glass bottles were generated per day in 2015 [3]. Based on the European Container Glass Federation statistic [4], the average recycling rate of container glass in Europe has reached 74% in 2014 and most of them were reused for manufacturing new glass. But in Hong Kong, most of the waste glass containers were disposed of in landfills rather than being recycled due to a lack of a local glass manufacturing industry. In order to enhance the recovery rate of waste glass beverage containers in Hong Kong, the Hong Kong Government has announced to implement a new mandatory Producer Responsibility Scheme on glass beverage containers [5], to provide support in waste glass recycling. Therefore, efforts need to be taken to explore potential strategies with a view to broadening the applications of recovered waste glass.

Recently there has been an increasing interest in recycling waste glass for the production of cement-based construction materials. Generally, the main attention has been focused on the use of recycled glass as a replacement of aggregates or cement in concrete and mortar.

For the incorporation of waste glass as aggregates replacement in concrete/mortar, there are contradictory opinions about the influence of glass aggregates on the workability. Several researchers [6-8] found that slump value of fresh concrete was reduced with an increasing percentage of glass aggregates. They attributed this behavior to the edged and angular grain shapes of the glass aggregates impeding the flow of the cement paste. Furthermore, additional cement paste was needed to coat the irregular glass aggregates resulting in less available cement paste for the fluidity. On the contrary, some investigators [9-11] reported that the replacement of natural aggregates by waste glass led to an improvement of workability due to the non-absorbent nature of glass. Moreover, severe bleeding and segregation occurred when 100% fine aggregates were replaced by recycled glass aggregates [12]. According to the study of Castro and De Brito [13], the different impacts of the glass aggregates on workability may be due to the workability was highly dependent on the particle size of the aggregates replaced. In terms of mechanical properties, the increasing contents of glass aggregates were reported to decrease the compressive, flexural strengths [7,14] and splitting tensile strength [15,16] of concrete. The reduction of strengths was also observed in the case of cement mortar with a high content of glass aggregates [10,17]. The possible reason was thought to be the presence of micro-cracks in the glass aggregates during the crushing process and the smooth surface of waste glass, which resulted in weaker bond strength between the glass surface and the cement paste.

With respect to the durability of glass cement-based materials, the inclusion of glass aggregates effectively improved the surface resistivity and sulfate attack with increased amounts of glass sand replacement [7]. The chloride ion penetrability and drying shrinkage of concrete decreased when the glass aggregates content increased [18]. However, because of the presence of a high amount of amorphous silica in waste glass, it cannot be used as aggregates without taking alkali-silica-reaction (ASR) problem into account. In recent years,

preventive actions were taken to mitigate the detrimental ASR expansion by incorporating fly ash [18,19], metakaolin [19,20], ground blast furnace slag [20,21], silica fume [22,23], glass powder [20,24], steel fiber [23], lithium nitrate [25].

The influence of waste glass powder as cement replacement on the properties of the cement-based materials has been extensively studied. According to a recent study by Lu et al. [26], the workability of architectural mortar was highly dependent on the particle size and morphology of the glass powder used. It was found that larger particle sized glass powder resulted in a reduction of the flow and the finer glass powder contributed to improving the workability. The reason was attributed to the fact that the larger and irregular glass particles could hinder the movement of the paste, while the finer glass powder could optimize the gradation of the mixture and reduce the friction between the particles. Many studies had been carried out to evaluate the mechanical properties of concrete containing glass powder, which has been proved to possess some pozzolanic activity [27-29]. The chemical compositions [30] and fineness [31] of glass powder were considered as important factors governing the reactivity of glass powder. From the study of Bignozzi et al. [30], the funnel and soda lime glass exhibited higher pozzolanic activity than the fluorescent lamps and crystal glass. Generally, the finer the particle size of glass powder, the higher was the strength of cement-glass blends [27,28,32]. However, replacement of cement by glass powder decreased the early compressive strength, although it increased the later compressive strength [33,34]. Several studies also reported that the compressive strength increased to a desired level up to a certain percentage of replacement and then decreased. Soliman et al. [34] stated that the optimum percentage of glass powder addition was 20% in ultra-high-performance concrete. Afshinnia et al. [33] and Aliabdo et al. [35] observed that inclusion of 10% of glass powder was considered to be optimum. In addition, from the study of Omran and his colleagues [36], incorporation of glass powder in concrete improved the long-term mechanical performance (compressive strength, splitting-tensile strength, flexural strength, and elastic modulus) as a result of the pozzolanic activity of the glass powder and the enhancement of the microstructure. As far as durability is concerned, the replacement of cement by glass powder in concrete or mortar could significantly improve the resistance to chloride-ion permeability [36-38], water penetration [39], sulfuric acid attack [40], freeze–thaw cycles [41] and ASR expansion [20,24,42]. Also, Kamali and Ghahremaninezhad [43] reported that the glass powder could significantly improve the electrical resistivity of cement paste compared to the control cement paste and fly ash blended cement paste, which was probably attributed to the pore refinement in the microstructure resulting from the pozzolanic reaction of glass powder.

However, most of the above-mentioned studies focused on investigating the effect of using glass as a cement or as an aggregate replacement individually on the properties of concrete/mortar. Few studies have been done to study the simultaneous use of glass aggregates and powder for the production of cement-based construction products [20,44]. Therefore, this study aimed to design an architectural mortar combining the use of glass

aggregates and powder and utilize the glass powder to counteract some drawbacks of the glass aggregates in the architectural mortar. . On the basis of waste glass recycling, it would be more effective to jointly use the waste glass in powder form as a cementitious material and in cullet form as aggregates. Furthermore, a novel channel for the recycling of mixed glass is to reuse it in architectural mortars/tiles so that the aesthetic appearance can be enhanced by taking into the advantage of the appealing colors of the waste glass cullet. This glass-based architectural mortar/tile for decorative applications (as shown in Fig. 1) is expected to replace the epoxy-based materials, which is not environmentally-friendly and has poor resistance to high temperature. Therefore, the objective of this work was to study the feasible use of waste glass powder to improve the durability of architectural mortar containing 100% glass aggregates. The influence of different particle sizes of glass powder on the durability of glass-based architectural mortar has been evaluated in terms of drying shrinkage, high temperature exposure resistance, sulfuric acid resistance and ASR. A comparative evaluation was carried out between the durability of glass-based mortar prepared with glass powder and fly ash.

Fig. 1 Architectural mortar produced with waste glass cullet and glass powder

2 Experimental details

2.1 Materials

2.1.1 Cementitious materials

For aesthetic reasons, white Portland cement (TAIHEIYO Cement Corp., Japan) was used as the main cementitious material to produce the architectural mortar. Glass powders (GP) with different fineness were collected after grinding the mixed glass cullet (GC) with a laboratory ball mill for 0.5 hour, 1 hour, 2 hours and 4 hours (namely as GP0.5h, GP1h, GP2h, GP4h), respectively. Fly ash (FA) was sourced from a local

coal-fired power plant. The chemical compositions of cement, GP and FA were determined by X-ray Florescence spectroscopy and the results are given in Table 1. The particle size distributions of cement, GP and FA were measured by a laser diffraction method (Malvern Instrument's Spraytec) and are shown in Fig. 2. As regards the surface morphology, a comparison of GP2h to FA is presented in Fig. 3. The scanning electronic micrographs indicate that the GP exhibits a smooth surface texture and irregular shape, while the FA is composed of spherical particles in micrometer order.

Table 1

Chemical compositions of cement, GP and FA (*wt* %).

	Cement	GP	FA
SiO_2	21.36	73.5	45.70
Al_2O_3	5.27	0.73	19.55
Fe_2O_3	0.20	0.38	11.72
CaO	67.49	10.48	12.27
MgO	1.14	1.25	4.10
K_2O	0.077	0.69	1.71
Na_2O	0.048	12.74	1.36
TiO_2	0.14	0.087	1.09
SO_3	2.60	-	1.82
$SiO_2 + Al_2O_3 + Fe_2O_3$	26.83	74.61	76.97

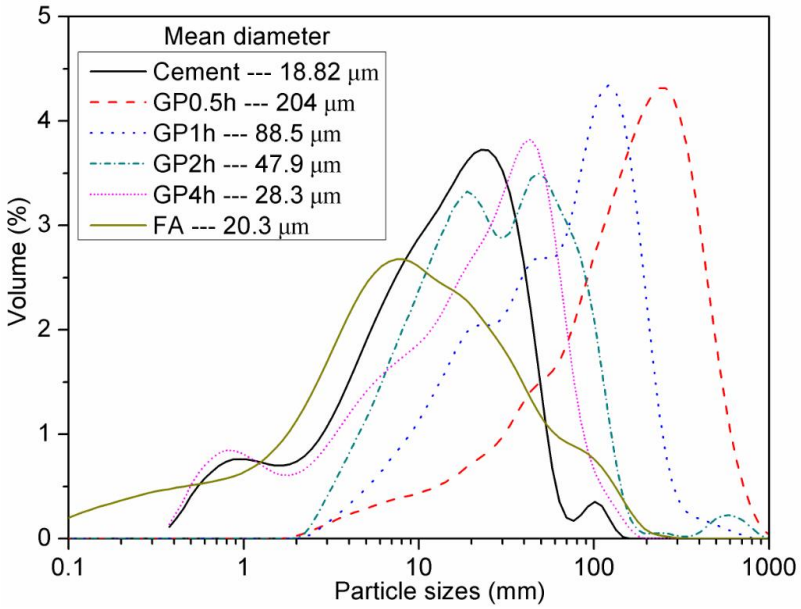

Fig. 2 Particle size distributions of cement, GP and FA

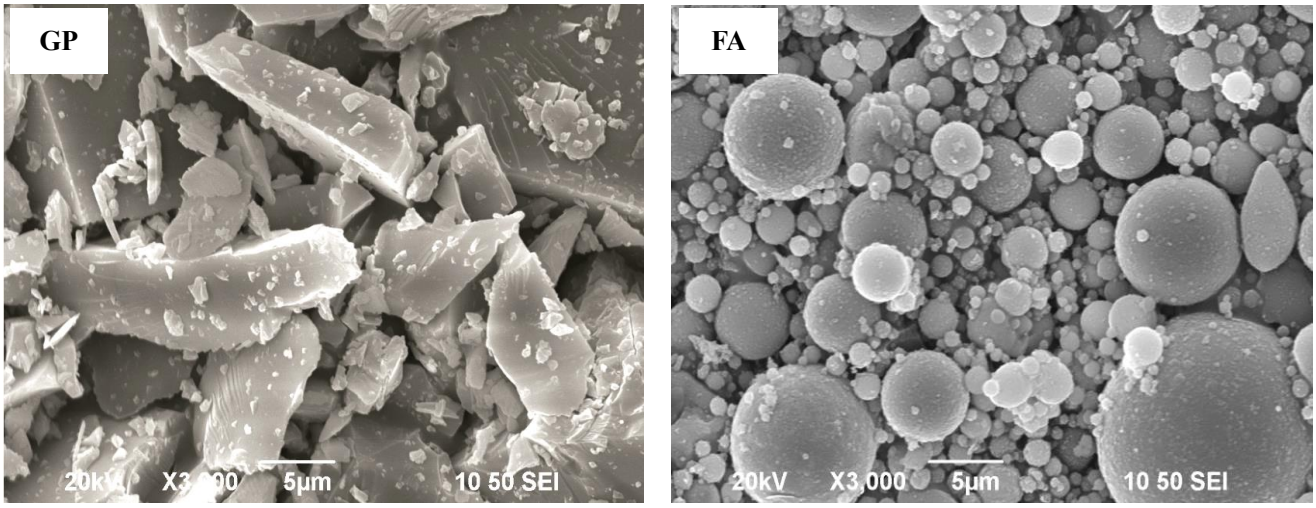

Fig. 3 Morphology of GP and FA

140
141

142 2.1.2 Aggregates

143 The fine aggregates used in this study was recycled GC with a mixed color which was obtained from a glass
144 waste recycling facility in Hong Kong. The waste GC was derived from crushing of collected post-consumer
145 beverage bottles. Before use, the GC was rinsed with tap water and oven-dried at 105 ºC for a minimum of
146 24h to remove contaminants and moisture. The appearance and gradation of GC are shown in Fig. 4. The
147 water absorption value, specific gravity and fineness modulus of this GC are 0.13%, 2.536 and 3.54,
148 respectively.

149

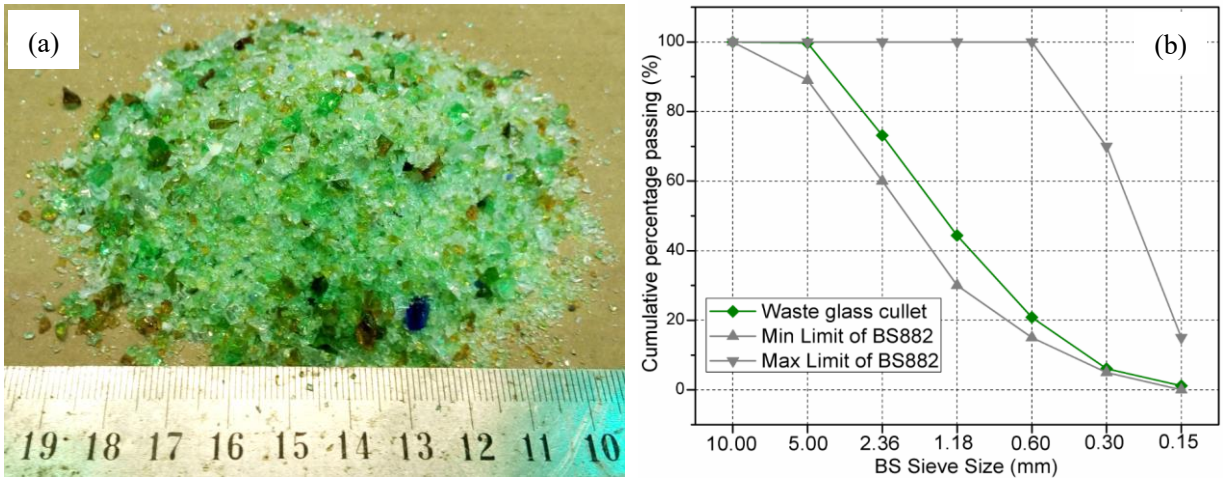

Fig. 4 Image (a) and gradation curve (b) of waste GC

150
151

152 **2.2 Mix proportioning for mortar preparation**

153 The mix proportions of GP and FA blended mortar mixtures are shown in Table 2. GP and FA were introduced
154 as supplementary cementitious materials at a replacement level of 20% by cement weight. It should be noted

that the architectural mortar prepared in this study contained more than 70% waste glass by dry mass (in glass cullet and powder forms in total). The cement mortar mixtures were prepared with a water-to-binder ratio of 0.4 and aggregate-to-binder ratio of 2.0. A superplasticizer (SP) ADVA-109 (W. R. Grace) was used to achieve the desired workability (flow values were above 210 mm). All the mixtures were mixed thoroughly before the fresh mortars were fabricated into molds followed by 15s vibration, and then demolded after 24h.

Table 2

Mix proportions of different mixtures (kg/m^3).

Mix	Cement	GP0.5h	GP1h	GP2h	GP4h	FA	GC	Water	SP
M-CON	706						1412	283	4.24
M-GP0.5h	565	141					1412	283	4.24
M-GP1h	565		141				1412	283	4.24
M-GP2h	565			141			1412	283	4.24
M-GP4h	565				141		1412	283	4.24
M-FA	565					141	1412	283	4.24

Note: M-CON stands for the control mortar with 100% white cement. The mortar mixtures named M-GP0.5h, M-GP1h, M-GP2h, M-GP4h and M-FA mean that 20% of cement used in the mortars were replaced with GP0.5h, GP1h, GP2h, GP4h and FA, respectively.

2.3 Test methods

2.3.1 Drying shrinkage

Three cement mortar prisms with size of 25 × 25 × 285 mm were prepared for testing of drying shrinkage according to a modified British Standard (BS ISO, Part 8: 1920) method [45]. The initial lengths were measured before the specimens were transferred to a drying chamber at 25 ºC and 50% relative humidity. Further measurements were carried out at the age of 1, 3, 7, 14, 28, 60, 90 days.

2.3.2 High temperature exposure resistance

For each mix, nine prisms (40× 40× 160 mm) were cast and then cured in a standard water curing tank. After 90 days of curing, three specimens were tested for initial flexural and compressive strength in conformity with ASTM C348 [46] and ASTM C349 [47], respectively. The other three specimens were oven dried at 105 ºC for 24h to remove free moisture. Then, the specimens were heated to 800 ºC at a heating rate of 5 ºC/min in an electric muffle furnace. After a 2h holding period, the furnace was switched off, allowing the samples to cool down to ambient temperature in the furnace before the residual flexural and compressive strength of samples were tested.

2.3.3 Acid resistance

The acid resistance of mortar samples was evaluated according to ASTM C 267 [48]. Three mortar prisms

(40 × 40 × 160 mm) were removed from water tank after 90 days of curing and the initial weight of each specimen was recorded under the saturated surface dried (SSD) condition. Then, all the specimens were immersed in a 3% H_2SO_4 solution. The weight measurements of the samples under SSD condition were taken weekly until 8 weeks. The acid solution was renewed every two weeks to maintain a stable acid concentration. The cumulative percentage mass change of each specimen was determined by the following formula:

$$\text{Cumulative mass change} = (M_t - M_i)/M_i \times 100\% \quad (1)$$

Where M_t is the mass of sample at immersion time t; M_i is the initial mass of sample before immersion in sulphuric acid.

2.3.4 ASR expansion

ASR expansion was measured on mortar prisms (25 × 25 × 285 mm) in accordance with ASTM C1260 [49]. After the specimens demolding (after casting for 24h), the mortar bars were transferred into a 80 ºC water tank for the next 24h. Then, a zero reading was taken within 15 ± 5 s after they were removed from the 80 ºC water tank. Afterward, the bars were immersed in 1 N NaOH solution at 80 ºC until the testing time. The expansion of the mortar bars was measured by using a length comparator. The measurements were conducted at the storage duration of 1, 4, 7, 14, 21 and 28 days.

2.3.5 Heat of hydration

The cement paste samples with the same formula in Table 2, but without addition of GC, were prepared for the determination of hydration heat by using an isothermal conduction calorimeter (Calmetrix I-CAL). Measurement of the heat of hydration in this study was carried out under an isothermal condition (20 ºC), and lasted for a period of 168h (7 days).

2.3.6 MIP

The accessible pore structures of mortars before and after subjecting to high temperature (800 °C) were evaluated by mercury intrusion porosimeter (MIP, Micromeritics AutoPore IV 9500 Series) with a maximum mercury intrusion pressure of 207 MPa. For the mortars without exposure to 800 °C, fractured samples were collected after testing the initial strength (section 2.3.2), and then the water in the samples was extracted by solvent exchange with anhydrous ethanol for one week, followed by drying in an oven at 60 °C for 3 days. For the preparation of mortar samples exposed to 800 °C, after completing the residual strength test (section 2.3.2), the fractured samples were immediately stored in sealed bottles until the MIP measurement. The porosity tested in this method was a wide range of pore sizes from 150 μm down to 7 nm. The mercury could only intrude the porosity that was interconnected and accessible from the outside. The volume of mercury penetrating a sample was measured as a function of increasing pressure (p), which was related to the diameter

(d) of the pores that had just been penetrated at that pressure by the equation: $p = 4\gamma \cos\theta/d$. Where γ is the surface tension of mercury and θ is advancing contact angle with the solid. This test used the usual assumption that the pores were cylindrical and θ was 140°.

2.3.7 TG

Thermogravimetric (TG) analyses were conducted on the mortar samples by using a Rigaku instrument (Thermo Plus Evo2 8121) in order to identify the phase compositions on the surface of the samples subjected in acid solution. After completing the acid corrosion test, the particles on the eroded surface (less than 3 mm) of the samples was scraped down and sieved, only the particles smaller than 300 μm were collected aiming to remove the coarse glass cullet as much as possible. Then, the collected powders were further ground until a grain size smaller than 75 μm was obtained. After oven-dried at 50 °C for 48h, the powdered samples were heated under atmosphere in the furnace, where the temperature was programmed to rise at a constant heating rate of 10 °C/min up to 1000 °C.

2.3.8 SEM-EDX

The samples for the morphology observations were collected after the ASR expansion test. Fragments from the crushed mortar specimens were collected and soaked into anhydrous ethanol for one week, followed by oven-drying at 60 ºC to remove the residual ethanol. Morphological observations and composition analysis were performed on the gold-coated samples using a scanning electron microscopy with energy dispersive X-ray spectroscopy (SEM-EDX, Tescan VEGA3).

3 Results and discussion

3.1 Drying shrinkage

Fig. 5 shows the influence of GP with different fineness and FA on the shrinkage of the glass-based mortar. It can be observed that the shrinkage values of the cement mortars were increased over time. However, the shrinkage values of the GP and FA blended mortars (approximate 500×10^{-6}) were obviously lower than that of the control mortar (729×10^{-6}). Moreover, most of the shrinkages on the cement mortars took place during the early ages (before 7 days of drying), especially for the control mortar without GP or FA. Therefore, the beneficial effect of reduction in shrinkage may be related to the dilution effect due to the addition of GP and FA. Incorporation of 20% GP or FA reduced the rate and degree of hydration and thus mitigated the reduction in volume of the solid phases due to the chemical reactions. This explanation is verified by the results of the heat of hydration test (Fig. 6), which shows that the cumulative heat of hydration was reduced as the GP or FA was used to replace cement. On the other hand, as expected, the introduction of GP and FA with lower reactivities and vitreous characteristics would result in higher effective water-to-cement ratios. According to

the works of Zhang et al. [50] and Lee et al. [51], the autogenous shrinkage decreased with increasing water-to-cement ratio. Therefore, the reduced total shrinkage could be partly attributed to the higher effective water-to-cement ratio resulting from the replacement of cement by GP and FA.

It is interesting to note that the effect of particle sizes of GP on the drying shrinkage of cement mortar was not significant, because the inclusion of GP with different particle sizes had little impact on hydration degree of cement-GP blends, as indicated by the curves of hydration heat in Fig. 6. This also explains why the drying shrinkage of the mortar sample with FA was broadly comparable to that of the samples with GP.

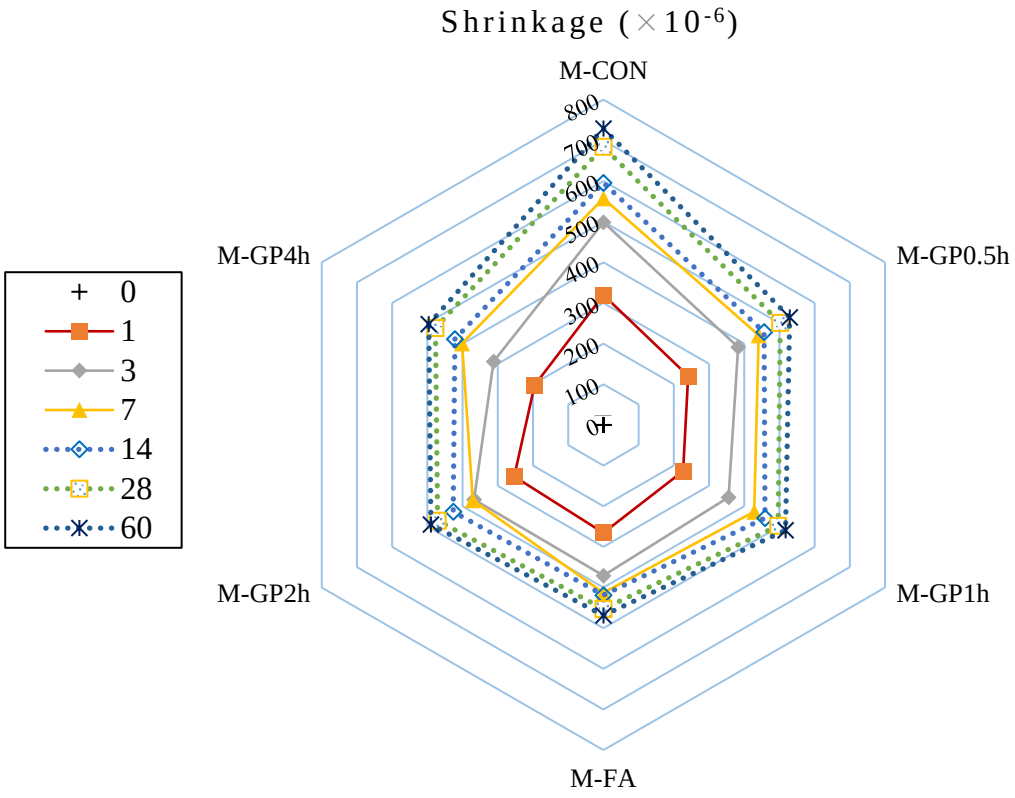

Fig. 5 Shrinkage of architectural mortars with GP and FA

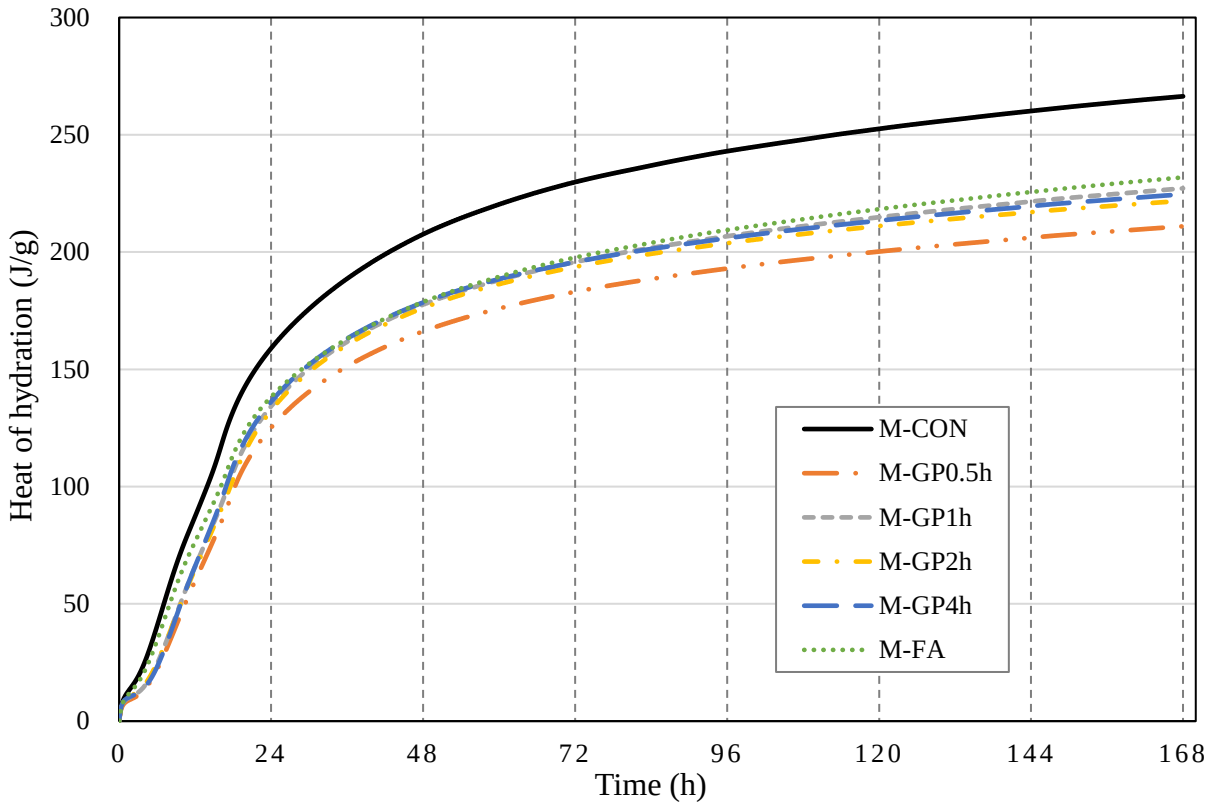

Fig. 6 Cumulative heat of hydration of cement pastes with GP and FA

265
266

267 **3.2 High temperature resistance**

268 The initial and residual strengths of the cement mortars subjected to 800 °C are illustrated in Figs. 7 and 8.
269 From the results of flexural strength (Fig. 7), it can be noted that the replacement of cement by GP brought
270 remarkable increase in the residual flexural strength as compared to the control mortar. Also, it is worth noting
271 that an increased trend was observed when the particle size of GP was decreased. This means that the fine GP
272 (GP2h and GP4h) had a greater contribution to improving the high temperature resistance. Although the initial
273 flexural strengths of the mortars prepared with the coarse GP (GP0.5h and GP1h) were lower than that of the
274 control mortar, the residual flexural strengths of former were higher than that of later, which indicates that the
275 positive effect due to the addition of GP was not attributed to the higher initial flexural strength. Furthermore,
276 regardless of the initial or residual flexural strength, the cement mortars prepared with fine GP had comparable
277 strength to the FA blended mortar.

278

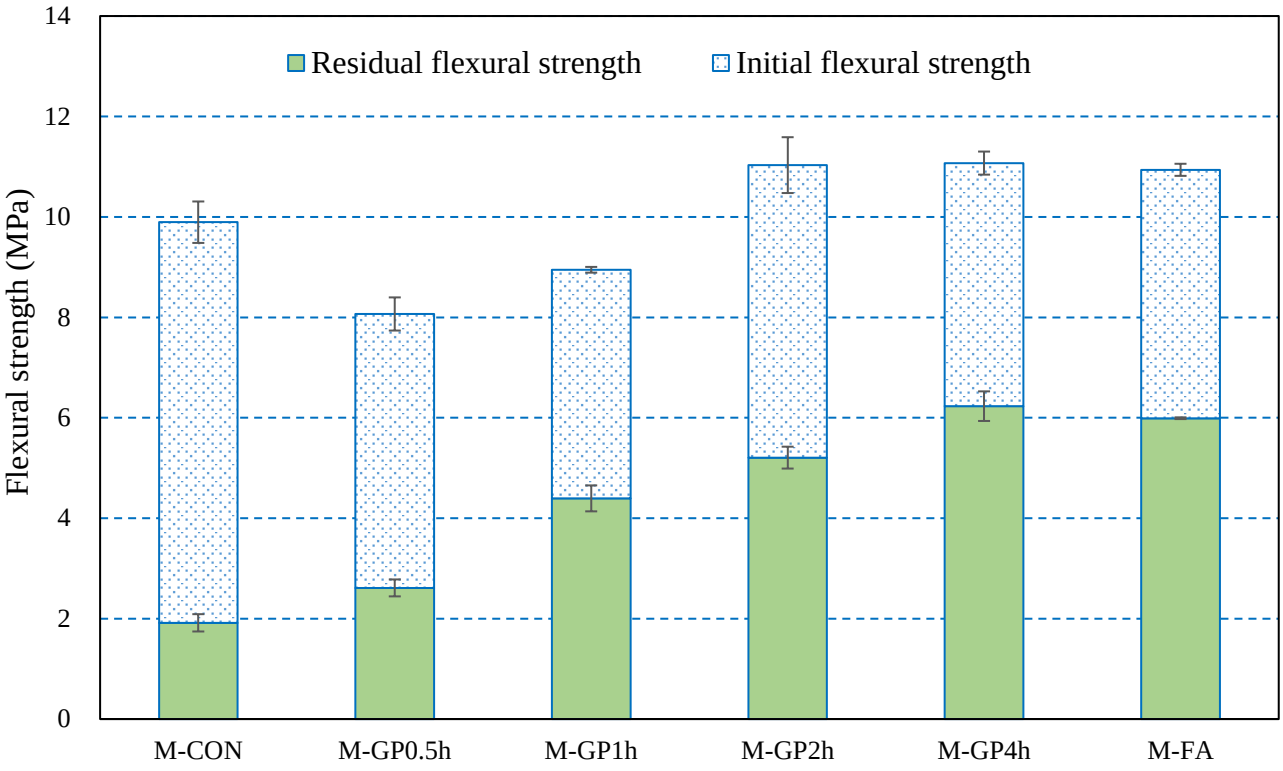

Fig. 7 Flexural strength of architectural mortars before and after exposure to 800 ºC

279

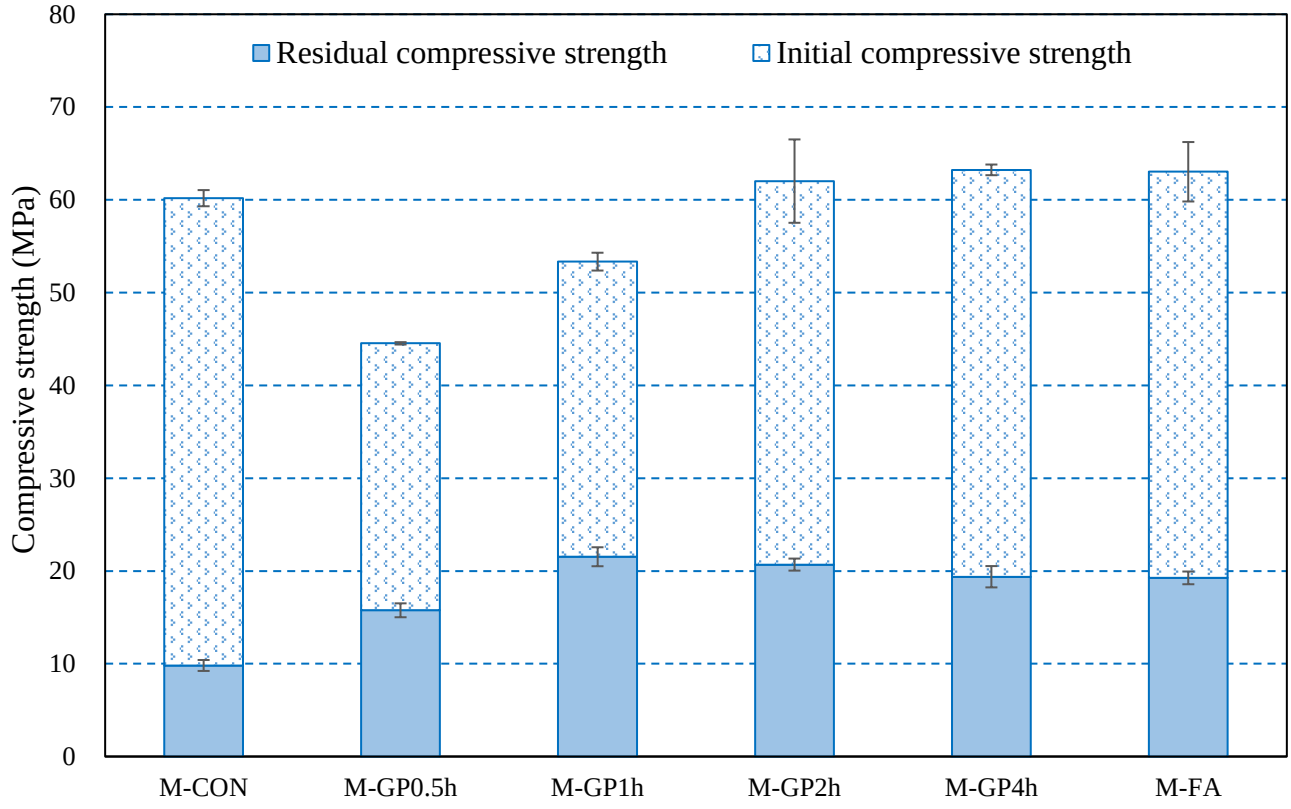

Fig. 8 Compressive strength of architectural mortars before and after exposure to 800 ºC

280

281

Fig. 8 illustrates variation in compressive strength of the architectural mortar. After exposure to 800 ºC, a drastic reduction of strength occurred for the control mortar. Peng and Huang [52] attributed the strength loss of concrete above 600 ºC to the decomposition of C–S–H. On the other hand, the different thermal expansion coefficients between the cement paste and the soda-lime glass aggregates may be another reason for the severe deterioration in strength [53]. However, the inclusion of fine GP (GP2h and GP4h) could significantly enhance the residual compressive strength although the fine GP blended mortars had similar initial compressive strength to the control mortar. Also, the GP blended mortars showed equivalent performance to the FA blended mortar after exposure to the high temperature. According to the study of Poon et al. [54], in the FA blended concrete, an improvement of pore structure at elevated temperatures was responsible for the higher relative residual compressive strength as compared to the pure cement concrete.

In order to understand the relationship between the microstructure of glass-based mortar after exposure to the high temperature and the corresponding strength loss, characteristics of pore structure were determined by using MIP (see Fig. 9). From the Fig. 9a, for the control mortar, a sharp increase in the average pore diameter was noticed due to the coarsening of the pore structure, which explains why the control mortar suffered severe strength loss after exposure to 800 ºC. Such pore structure coarsening was also verified by SEM observations [52]. However, significant decreases in the average pore diameter were observed in the mortars prepared with GP, indicating that the mitigation of coarsening effect of the pore structure was considered to be the result of the higher resistance to high temperature in the GP blended mortars. By contrast, a similar behavior occurred in the case of the mortar prepared with FA. These findings are also consistent with the results reported in a previous work [54].

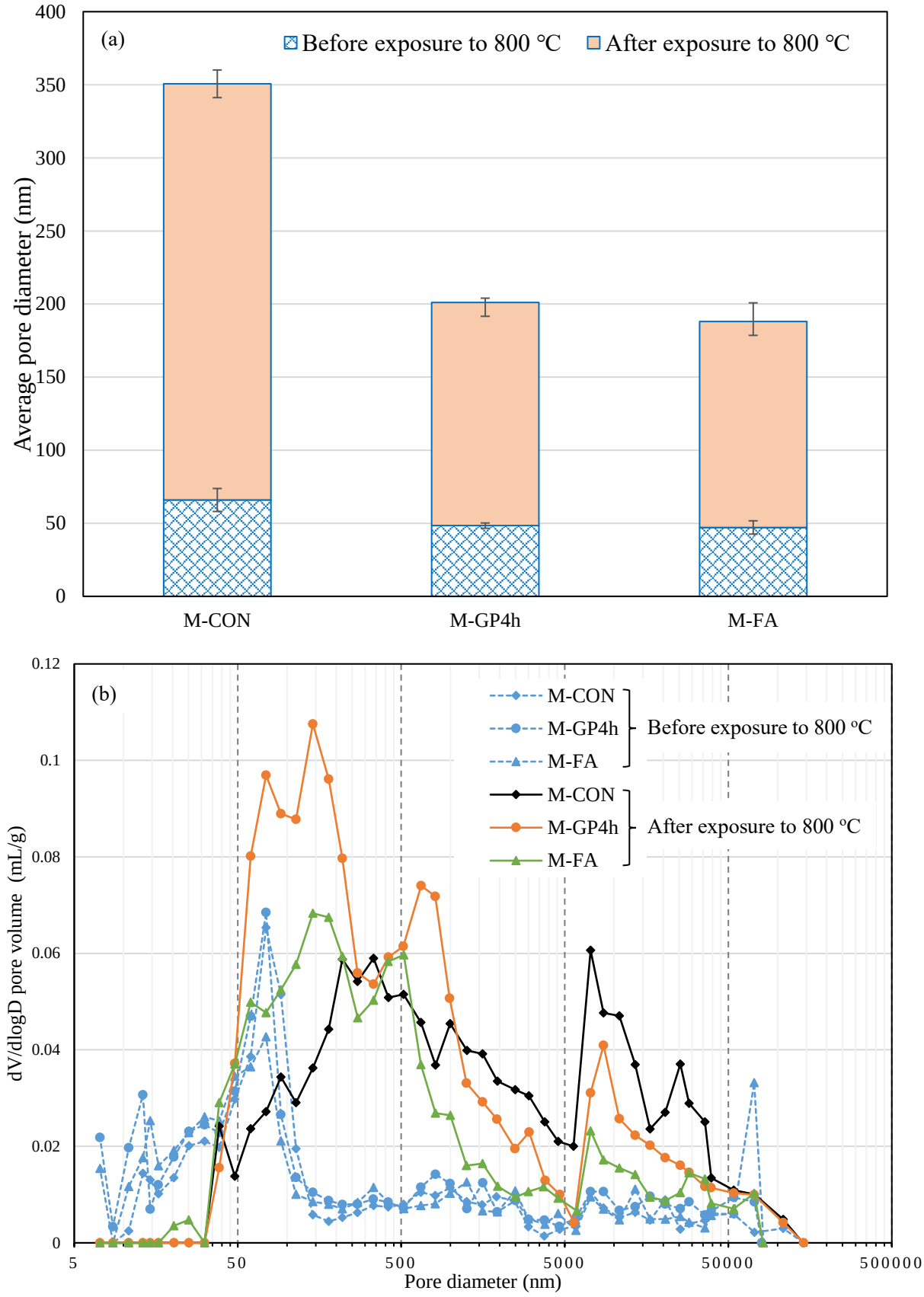

Fig. 9 Pore structure of architectural mortars before and after exposure to 800 ℃: Average pore diameters (a) and Differential pore size distributions (b)

The differential pore size distribution results for the mortars before and after exposure to 800 ºC are given in Fig. 9b, which intuitively shows the coarsening effect of the elevated temperature on the pore structure. Before exposure to 800 ºC, more micropores (＜50 nm) were observed in the GP and FA blended mortars compared to the control mortar due to the pozzolanic reaction of GP and FA. However, after heating to 800 ºC, such micropores almost disappeared. In addition, the maximum peaks (critical pore diameter) located at the pore diameter of about 70 nm shifted towards the right side after exposure to the high temperature, which means that the pore structure of mortars became coarser. Meanwhile, it can be seen that the amount of pore volumes of the capillary pores between 50 nm and 200 nm were higher in the GP and FA blended mortars than in the control mortar. This behavior is probably because the additional C–S–H gel derived from pozzolanic reaction of GP and FA was decomposed, and thus the gel pores and micropores (＜50 nm) changed to larger pore sizes.

Also, significant alterations were observed in the range of pore diameter larger than 1000 nm (mesopores and macropores). There were drastic increases after the mortars were subjected to the high temperature. The beneficial effect of the addition of GP and FA can be identified from the smaller volumes of the large pores in the blended mortars. Although the GP and FA blended mortars had larger numbers of fine pores (50~200 nm) when the temperature was elevated to 800 ºC, the lower proportion of larger pores (＞1000 nm) in the blended mortar were believed to be mainly responsible for the retention of strength. The reason for the mitigation of the pore size coarsening by GP and FA may be due to the fact that the incorporation of pozzolanic materials could reduce the thermal mismatch between the hardened cement paste and the aggregates [55].

3.3 Acid resistance

The mass changes of the cement mortars after immersion in the sulfuric acid solution are illustrated in Fig. 10. It is clearly seen that the mass of all the mortars samples were increased during the initial week. This phenomenon is consistent with the study of O'Connell et al. [56] and can be attributed to the formation of additional ettringite and gypsum on the surface of the mortars [57]. However, after 4 weeks of exposure to the acid, both the control mortar and FA blended mortars suffered rapid mass losses and similar cumulated mass losses were recorded after immersion for 8 weeks. For the control mortar, the hydration products (e.g. calcium hydroxide and C-S-H gel) could react with the sulfuric acid to form the expansive gypsum and ettringite, which would disintegrate the mortar structure due to the internal swelling stresses [58,59]. For the case of FA mortar, the effect of FA on sulfuric acid resistance was almost negligible, which is in agreement with the finding of ydın et al. [60].

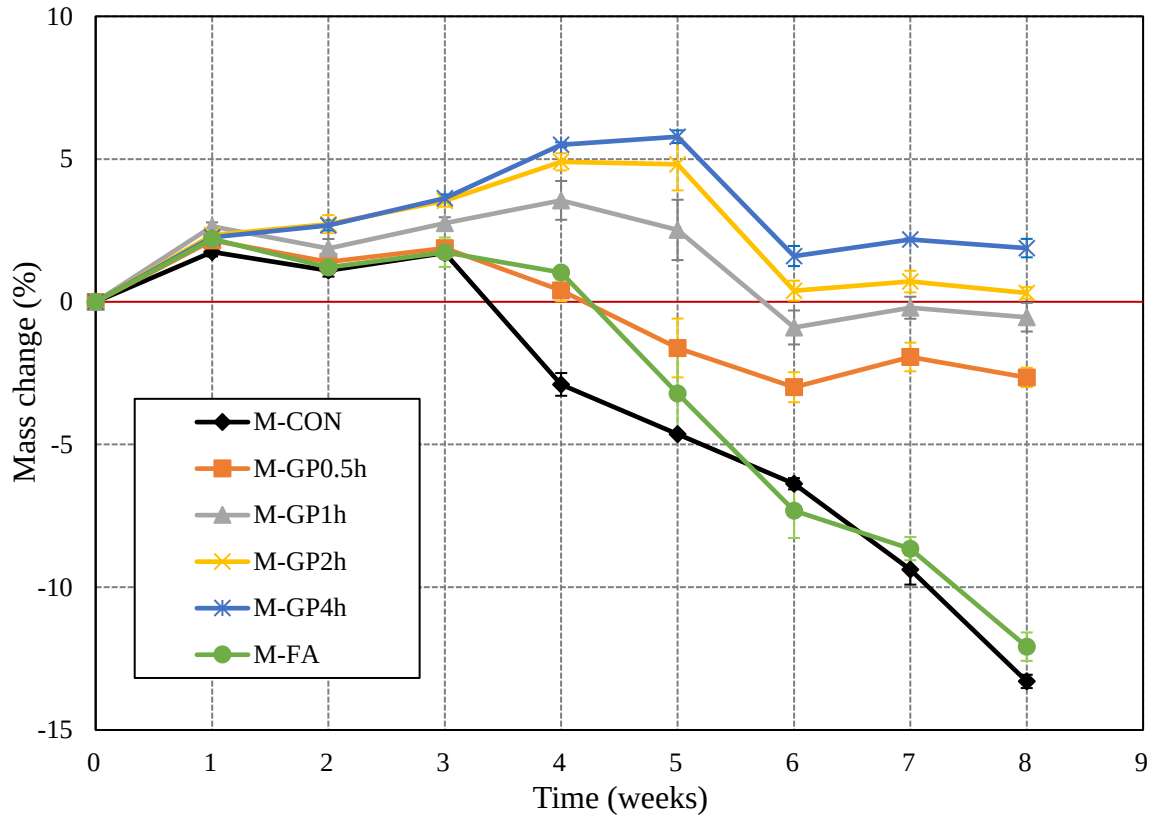

Fig. 10 Mass changes of architectural mortars with GP and FA

By comparison with the control and the FA specimens, the replacement of cement by GP effectively improved the resistance of the architectural mortar to the sulfuric acid attack; the finer the GP particles used, the more significant the improvements were. The mortars incorporating the coarse GP lost more than 2% of the initial mass after 8-week of immersion, while the final mass of mortars containing the fine GP even exceeded the initial mass before immersion. Sulfuric acid is particularly aggressive because not only the calcium hydroxide and C-S-H, but also aluminate phases would be decomposed by the acid attack [61]. Therefore, several aspects need to be taken into account for explaining the beneficial effects of GP on acid resistance: (i) the pozzolanic reaction of GP could consume large amount of calcium hydroxide, which is usually the most vulnerable cement hydration product with respect to acid attack [61]. Moreover, the formation of additional C-S-H enabled better resistance to the sulfuric acid [58]. (ii) the reduction of calcium hydroxide and aluminate phase contents due to the dilution effect reduced the amount of gypsum and ettringite formation, thus mitigated the development of expansive pressure. In order to verify this interpretation, the total amount of gypsum and ettringite remained in the eroded surface of the mortars after the sulfuric acid attack test was measured by thermogravimetry. Fig. 11 shows that the weight loss before 200 ºC (decomposition of gypsum and ettringite [62]) followed the order of fine GP blended mortar, FA blended mortar, control mortar, which corroborated well with the above discussion. (iii) the unreacted GP with a vitreous structure (as seen in Fig. 3) had a good resistance against acid attack [63].

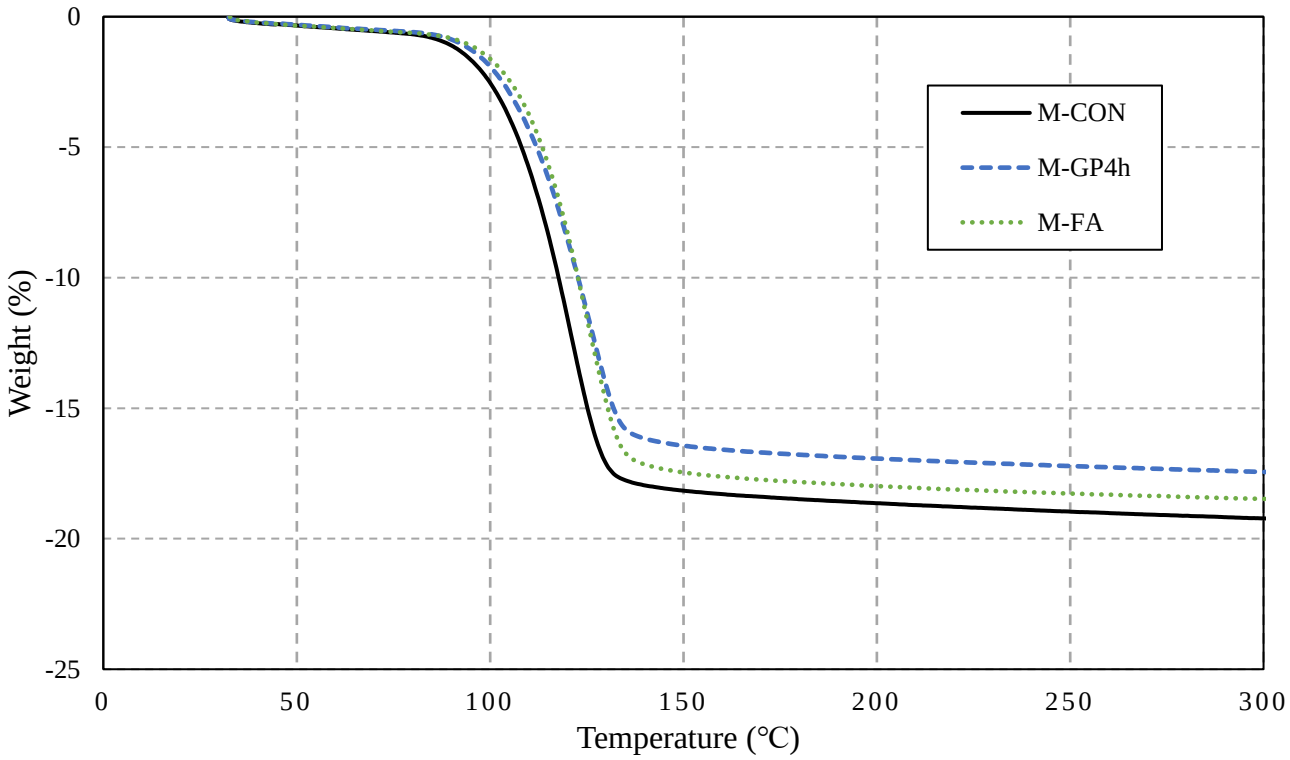

Fig. 11 Thermal analysis of architectural mortars after sulfuric acid attack

3.4 ASR

Fig. 12 shows that the influence of GP with different particle sizes and FA on the ASR expansion of the cement mortars. Apparently, the expansion rate of the control mortar at 14 days far exceeded the 0.1% limit specified by ASTM C1260 [49]. However, it can be noticed that the inclusion of GP and FA could effectively suppress the expansion due to the ASR. In addition, the rate of expansion was decreased with reducing the GP particle size used in the mortars. Also, it is worth noting that in this study all the aggregates were fully replaced by the GC, the replacement of 20% cement by fine GP (GP2h and GP4h) could successfully eliminate the deteriorative expansion caused by ASR of GC. Therefore, the results validate the feasibility of maximizing the utilization of waste glass in architectural mortars by jointly using GC as aggregates and GP as binders. When compared the case of M-GP4h to M-FA, it can be observed that GP behaved quite similarly to FA with regard to mitigation of ASR expansion. Although the test age was extended to 28 days, the ASR expansion rates of the fine GP and FA blended mortars still remained below the permissible limits (0.1%). SEM images taken on the GP and the FA specimens are shown in Fig 13. It can be observed that the microstructures of the samples show no signs of cracks due to ASR. However, as indicated in Fig. 13a, visible cracks are observed on the periphery of the GC in the case of the control mortar.

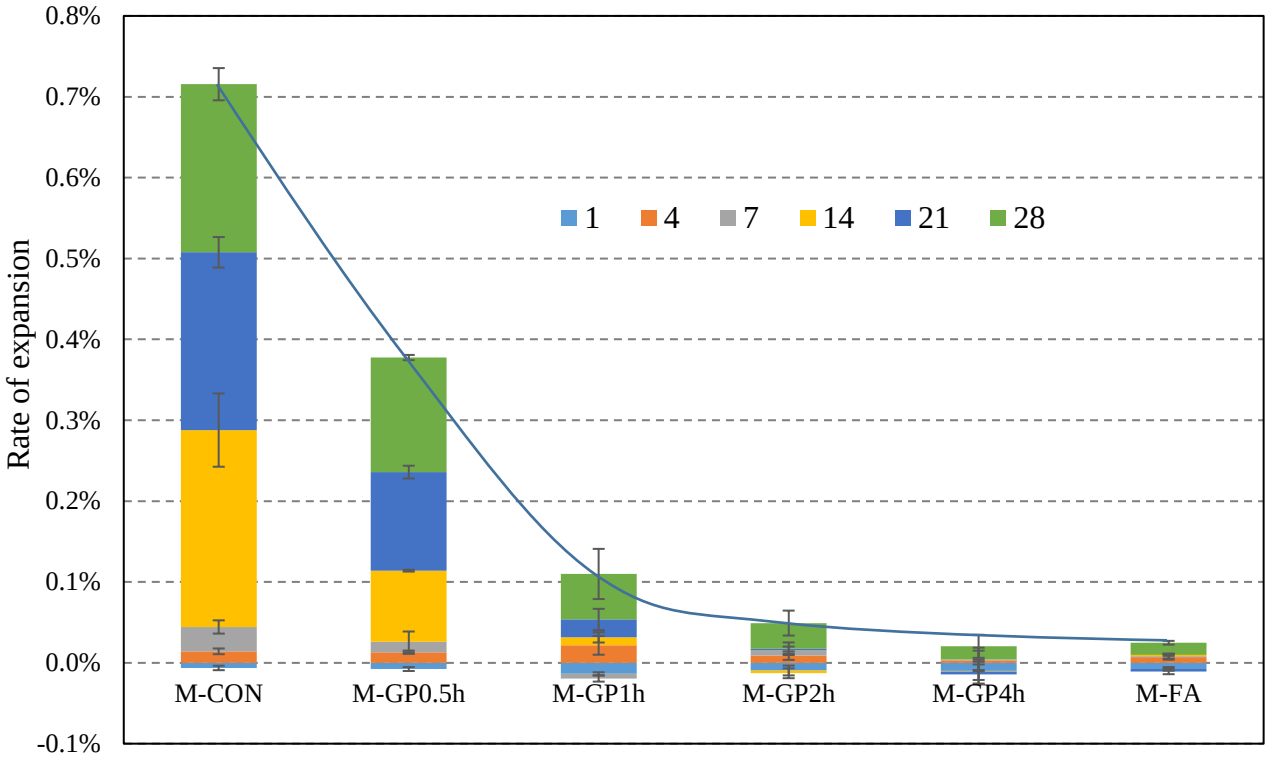

Fig. 12 ASR expansion of architectural mortars with GP and FA

377

378

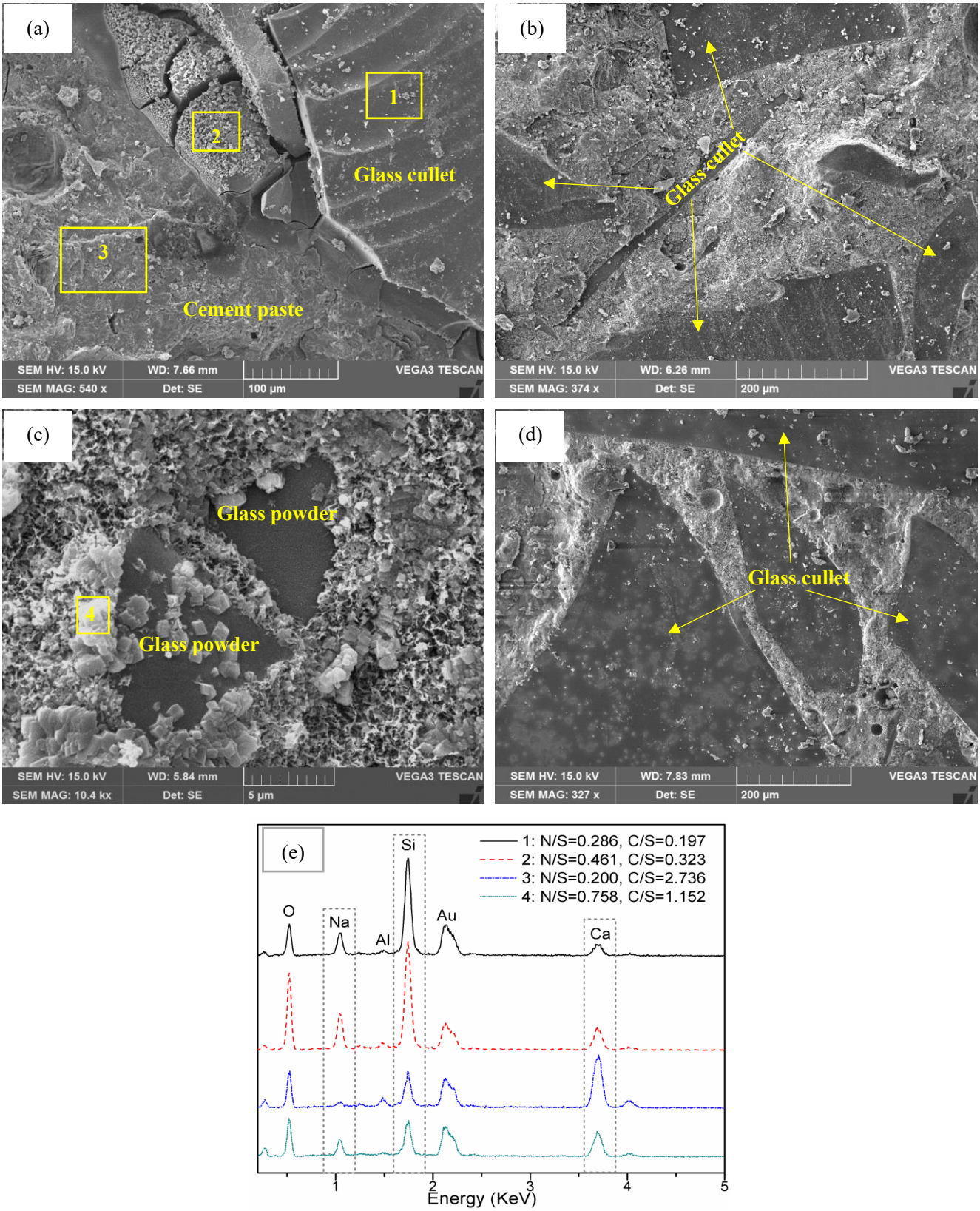

Fig. 13 SEM images and EDX spectrums of cement mortars (a) ASR damage in control mortar (b) absence of ASR cracks in M-GP4h mortar (c) pozzolanic reaction of GP (d) absence of ASR cracks in M-FA mortar (e) compositions of zone 1, 2, 3 and 4 by EDX.

379

380

Based on the EDX results (Fig. 13e) of zones 1 and 2 in Fig. 13(a), the reaction rim (zone 2) shows much higher Na/Si and Ca/Si ratios than the GC (zone 1). On the contrary, compared to the cement paste matrix (zone 3), the reaction rim had much lower calcium contents (Fig. 13e). It is believed therefore that these alkali-calcium-silicate products were the expansive ASR gel, which led to expansion by adsorption of water in the vicinity of GC. From Fig. 13c, the fine glass particles were eroded and formed additional products on the surface or around the rim of the glass particles. These secondary products were mainly due to the pozzolanic reaction between the GP and the calcium hydroxide. As evidenced by the EDX analysis (see Fig. 13e), the Ca/Si of the products was 1.152, indicating that the inclusion of GP in the mortar could significantly reduce the Ca/Si in the C-S-H in comparison with the zone 3. The high content of silica in the glass was responsible for the reduced Ca/Si ratio. Also, it is interesting to notice that the C-S-H contained a high amount of alkali (Na/Si was 0.758). According to the work of Monteiro et al. [64], C-S-H with low Ca/Si ratio had capacity to incorporate a significantly higher quantity of alkalis than normal C-S-H. Therefore, it can be deducted from the above that, the production of secondary C-S-H by addition of GP may partly contribute to mitigation of ASR expansion. Furthermore, due to the pozzolanic reaction, sufficient amounts of fine siliceous GP in the mortar could inhibit the ASR by absorbing most of Ca^{2+} ions, which were necessary for the formation of swelling gel [65-67]. Another explanation for the reduction of ASR expansion was proposed by Ichikawa [67], who pointed out that the rate of ASR was highly controlled by the particle size of the reactive aggregate, and the grain size less than 50 μm (large specific surface area) would preferentially react with alkali hydroxide to prevent the formation of expansive pressure after the formation of tight reaction rims. On the basis of this size effect, introduction of alkali-reactive GP with small particle size is thus expected to suppress ASR even when the mortar contained a certain amount of reactive glass aggregates. Because of the higher degree of pozzolanic reaction and smaller particle size, the finer GP was highly effective in preventing the deleterious expansion as compared to the coarser GP, which was also proven by the results of Idir et al. [24].

4 Conclusions

In this study, mixed color waste glass was employed to design a novel glass-based architectural mortar/tile. The waste glass was used in two forms (i.e. cullet and powder), which not only made use of the aesthetic nature of glass cullet as decorative aggregates, but also utilized its pozzolanic characteristic of the glass powder as a replacement of cement. Surprisingly, partially replacing cement by GP has positive influences on the durability performances of the architectural mortar containing 100% glass aggregates. The following conclusions are drawn based on the experimental results from this investigation:

The incorporation of GP in the glass-based mortar as a cement replacement significantly reduced the drying shrinkage. The reason may be related to the reduction of hydration degree due to the dilution effect. In addition,

the impact of particle size of GP on the drying shrinkage was insignificant due to the similar degree of hydration achieved. When exposed to high temperature, the replacement of cement by GP in the glass-based mortar brought remarkable increases in the residual flexural and compressive strength as compared to the control mortar. Furthermore, the fine GP (＜50 μm) had greater contribution to enhancing the resistance to high temperature exposure due to the mitigation of coarsening effect on the pore structure. By comparison with the control and FA mortar, the inclusion of GP effectively improved the resistance of glass-based mortar to the sulfuric acid attack. In addition, the positive effect was more pronounced when the particle size of GP was reduced. The replacement of 20% cement by fine GP (＜50 μm) could successfully mitigate the deteriorative ASR expansion caused by the glass aggregates. Due to the higher degree of pozzolanic reaction and size effect, the finer GP was highly effective in preventing the expansion as compared to the coarser GP. In conclusion, the durability performance of the architectural mortar prepared with 100% glass aggregates were improved with decreasing the particle size of GP. Especially, the properties of architectural mortar incorporating GP with a particle size of less than 50 μm were comparable or even superior to those of the architectural mortar containing traditional supplementary cementitious material (i.e. FA). Moreover, unlike FA, the nearly white color of GP would not stain the aesthetic appearance of architectural mortar. Consequently, it is feasible to jointly using waste GP to partially replace white cement and waste GC as aggregates for the production of architectural mortars/tiles with good durability. Compared with previous works, this study extended the application of waste glass both as a decorative material and a pozzolanic material to a much larger volume (more than 70%) in the architectural mortars/tiles.

Acknowledgement

The authors wish to thank the financial support of The Hong Kong Polytechnic University (Project of Strategic Importance).

Reference

[1] E.L. Bourhis, Glass: mechanics and technology, Wiley-VCH, Weinheim, 2008.
[2] J.E. Shelby, Introdution to glass science and technology, 2nd edition.
[3] Environmental Protection Department (EPD). Monitoring of solid waste in Hong Kong (Waste Statistics for 2015): https://www.wastereduction.gov.hk/sites/default/files/msw2015.pdf.
[4] European Container Glass Federation (FEVE): http://feve.org/glass-packaging-closed-loop-recycling-74-eu/.
[5] Environmental Protection Department (EPD). Producer Responsibility Schemes: http://www.epd.gov.hk/epd/english/environmentinhk/waste/pro_responsibility/index.html)
[6] S.B. Park, B.C. Lee, J.H. Kim, Studies on mechanical properties of concrete containing waste glass

aggregate, Cem. Concr. Res. 34 (2004) 2181–2189.
[7] H.Y. Wang, A study of the effects of LCD glass sand on the properties of concrete, Waste Manage. 29 (2009) 335–341.
[8] Z.Z. Ismail, E.A. AL-Hashmi, Recycling of waste glass as a partial replacement for fine aggregate in concrete, Waste Manage. 29 (2009) 655–659.
[9] H. Zhao, C.S. Poon, T.C. Ling, Properties of mortar prepared with recycled cathode ray tube funnel glass sand at different mineral admixture, Constr. Build. Mater. 40 (2013) 951–960.
[10] T.C. Ling, C.S. Poon, S.C. Kou, Feasibility of using recycled glass in architectural cement mortars, Cem. Concr. Compos. 33 (2011) 848–854.
[11] M.J. Terro, Properties of concrete made with recycled crushed glass at elevated temperatures, Build. Environ. 41 (5) (2006) 633–639.
[12] B. Taha, G. Nounu, Properties of concrete contains mixed colour waste recycled glass as sand and cement replacement, Constr. Build. Mater. 22 (2008) 713–720.
[13] S. de Castro, J. de Brito, Evaluation of the durability of concrete made with crushed glass aggregates, J. Clean. Prod. 41 (2013) 7–14.
[14] İ.B. Topçu, M. Canbaz, Properties of concrete containing waste glass, Cem. Concr. Res. 34 (2004) 267–274.
[15] A. Mardani-Aghabaglou, M. Tuyan, K. Ramyar, Mechanical and durability performance of concrete incorporating fine recycled concrete and glass aggregates, Mater. Struct. (2015) 48:2629–2640.
[16] T.C. Ling, C.S. Poon, Feasible use of recycled CRT funnel glass as heavyweight fine aggregate in barite concrete, J. Clean. Prod. 33 (2012) 42–49.
[17] K.H. Tan, H.J. Du, Use of waste glass as sand in mortar: Part I – Fresh, mechanical and durability properties, Cem. Concr. Compos. 35 (2013) 109–117
[18] S.C. Kou, C.S. Poon, Properties of self-compacting concrete prepared with recycled glass aggregate, Cem. Concr. Compos. 31 (2009) 107–113.
[19] C.S. Lam, C.S. Poon, D. Chan. Enhancing the performance of pre-cast concrete blocks by incorporating waste glass – ASR consideration, Cem. Concr. Compos. 29 (2007) 616–625.
[20] B. Taha, G. Nounu, Utilizing waste recycled glass as sand/cement replacement in concrete, J. Mater. Civ. Eng. 21(12) (2009) 709–721.
[21] T.C. Ling, C.S. Poon, Feasible use of large volumes of GGBS in 100% recycled glass architectural mortar, Cem. Concr. Compos. 53 (2014) 350–356.
[22] A. Shayan, A. Xu, Value-added utilisation of waste glass in concrete. Cem. Concr. Res. 34 (2004) 81–9.
[23] H.J. Du, K.H. Tan, Use of waste glass as sand in mortar: Part II – Alkali–silica reaction and mitigation methods, Cem. Concr. Compos. 35 (2013) 118–126.
[24] R. Idir, M. Cyr, A. Tagnit-Hamou, Use of fine glass as ASR inhibitor in glass aggregate mortars, Constr. Build. Mater. 24 (2010) 1309–1312.

[25] B. Taha, G. Nounu, Using lithium nitrate and pozzolanic glass powder in concrete as ASR suppressors, Cem. Concr. Compos. 30 (2008) 497–505.
[26] J.X. Lu, D.Z. Hua, C.S. Poon. Fresh properties of cement pastes or mortars incorporating waste glass powder and cullet, Constr. Build. Mater. 131 (2017) 793–799.
[27] Y.X. Shao, T. Leforta, S. Morasa, D. Rodriguez, Studies on concrete containing ground waste glass, Cem. Concr. Res. 30 (2000) 91–100.
[28] C.J. Shi, Y.Z. Wu, C. Riefler, H. Wang, Characteristics and pozzolanic reactivity of glass powders, Cem. Concr. Res. 35 (2005) 987–993.
[29] N. Schwarz, N. Neithalath, Influence of a fine glass powder on cement hydration: Comparison to fly ash and modeling the degree of hydration, Cem. Concr. Res. 38 (2008) 429–436.
[30] M.C. Bignozzi, A. Saccani, L. Barbieri, I. Lancellotti, Glass waste as supplementary cementing materials: The effects of glass chemical composition, Cem. Concr. Compos. 55 (2015) 45–52.
[31] M. Mirzahosseini, K.A. Riding, Influence of different particle sizes on reactivity of finely ground glass as supplementary cementitious material (SCM), Cem. Concr. Compos. 56 (2015) 95–105.
[32] J.X. Lu, Z.H. Duan, C.S. Poon, Combined use of waste glass powder and cullet in architectural mortar, Cem. Concr. Compos. 82 (2017) 34–44.
[35] K. Afshinnia, P.R. Rangaraju, Influence of fineness of ground recycled glass on mitigation of alkali–silica reaction in mortars, Constr. Build. Mater. 81 (2015) 257–267.
[34] N.A. Soliman, A. Tagnit-Hamou, Development of ultra-high-performance concrete using glass powder–Towards ecofriendly concrete, Constr. Build. Mater. 125 (2016) 600–612.
[35] A.A. Aliabdo, A.E.M.A. Elmoaty, A.Y. Aboshama, Utilization of waste glass powder in the production of cement and concrete, Constr. Build. Mater. 124 (2016) 866–877.
[36] A.F. Omran, E. D.-Morin, D. Harbec, A. Tagnit-Hamou, Long-term performance of glass-powder concrete in large-scale field applications, Constr. Build. Mater. 135 (2017) 43–58.
[37] A.M. Matos, J. Sousa-Coutinho, Durability of mortar using waste glass powder as cement replacement, Constr. Build. Mater. 36 (2012) 205–215.
[38] M. Kamali, A. Ghahremaninezhad, Effect of glass powders on the mechanical and durability properties of cementitious materials, Constr. Build. Mater. 98 (2015) 407–416.
[39] H.J. Du, K.H. Tan, Waste glass powder as cement replacement in concrete, J. Adv. Concr. Tech. 12 (2014) 468–477.
[40] H. Siad, M. Lachemi, M. Sahmaran, K.M.A. Hossain, Effect of glass powder on sulfuric acid resistance of cementitious materials, Constr. Build. Mater. 113 (2016) 163–173.
[41] A. Omran, A. Tagnit-Hamou, Performance of glass-powder concrete in field applications, Constr. Build. Mater. 109 (2016) 84–95.
[42] N. Schwarz, H. Cam, N. Neithalath, Influence of a fine glass powder on the durability characteristics of concrete and its comparison to fly ash, Cem. Concr. Compos. 30 (2008) 486–496.

[43] M. Kamali, A. Ghahremaninezhad, An investigation into the hydration and microstructure of cement pastes modified with glass powders, Constr. Build. Mater. 112 (2016) 915–924.
[44] K. Afshinnia, P.R. Rangaraju, Impact of combined use of ground glass powder and crushed glass aggregate on selected properties of Portland cement concrete, Constr. Build. Mater. 117 (2016) 263–272.
[45] BS ISO 1920-8. Determination of drying shrinkage of concrete for samples prepared in the field or in the laboratory. British Standard Institution; 2009.
[46] ASTM C348. Standard test method for flexural strength of hydraulic-cement mortars. American Society of Testing Materials; 2008.
[47] ASTM C349. Standard test method for compressive strength of hydraulic-cement mortars (using portions of prisms broken in flexure). American Society of Testing Materials; 2008.
[48] ASTM C 267. Standard test methods for chemical resistance of mortars, grouts, and monolithic surfacings and polymer concretes. American Society of Testing Materials; 2001.
[49] ASTM C 1260. Standard test method for potential alkali reactivity of aggregates (mortar-bar method). American Society of Testing Materials; 2007.
[50] M.H. Zhang, C.T. Tam, M.P. Leow, Effect of water-to-cementitious materials ratio and silica fume on the autogenous shrinkage of concrete, Cem. Concr. Res. 33 (2003) 1687–1694.
[51] K.M. Lee, H.K. Lee, S.H. Lee, G.Y. Kim, Autogenous shrinkage of concrete containing granulated blast-furnace slag, Cem. Concr. Res. 36 (2006) 1279–1285.
[52] G.F. Peng, Z.S. Huang, Change in microstructure of hardened cement paste subjected to elevated temperatures, Constr. Build. Mater. 22 (2008) 593–599.
[53] J.X. Lu, B.J. Zhan, Z.H. Duan, C.S. Poon, Improving the performance of architectural mortar containing 100% recycled glass aggregates by using SCMs, Accepted by Constr. Build. Mater. (2017).
[54] C.S. Poon, S. Azhar, M. Anson, Y.L. Wong, Comparison of the strength and durability performance of normal-and high-strength pozzolanic concretes at elevated temperatures, Cem. Concr. Res. 31 (2001) 1291–1300.
[55] Z.H. Shui, R. Zhang, W. Chen, D.X. Xuan, Effects of mineral admixtures on the thermal expansion properties of hardened cement paste, Constr. Build. Mater. 24 (2010) 1761–1767.
[56] M. O'Connell, C. McNally, M.G. Richardson, Performance of concrete incorporating GGBS in aggressive wastewater environments, Constr. Build. Mater. 27 (1) (2012) 368–374.
[57] Z. Makhloufi, E.H. Kadri, M. Bouhicha, A. Benaissa, Resistance of limestone mortars with quaternary binders to sulfuric acid solution, Constr. Build. Mater. 26 (1) (2012) 497–504.
[58] F. Girardi, W. Vaona, R. Di Maggio, Resistance of different types of concretes to cyclic sulfuric acid and sodium sulfate attack, Cem. Concr. Compos. 32 (2010) 595–602.
[59] D.M. Roy, P. Arjunan, M.R. Silsbee, Effect of silica fume, metakaolin, and low-calcium fly ash on chemical resistance of concrete, Cem. Concr. Res. 31 (12) (2001) 1809–1813.
[60] S. Aydın, H. Yazıcı, H. Yiğiter, B. Baradan, Sulfuric acid resistance of high-volume fly ash concrete,

Build. Environ. 42 (2007) 717–721.
[61] A.M. Neville, Properties of concrete, John Wiley and Sons Inc., New York, 1996.
[62] N.C. Collier, Transition and decomposition temperatures of cement phases–a collection of thermal analysis data, Ceramics-Silikaty, 0 (4) (2016) 338–343
[63] I. Fanderlik, Silica glass and its application, Elsevier Science Publishing Company, INC, New York, 1991.
[64] P.J.M. Monteiro, K. Wang, G. Sposito, M.C. dos Santos, W.P. de Andrade, Influence of mineral admixtures on the alkali-aggregate reaction, Cem. Concr. Res. 27 (12) (1997) 1899–1909.
[65] H. Wang, J.E. Gillott, Mechanism of alkali–silica reaction and the significance of calcium hydroxide, Cem. Concr. Res. 21 (1991) 647–654.
[66] X.Q. Hou, L.J. Struble, R.J. Kirkpatrick, Formation of ASR gel and the roles of C-S-H and portlandite, Cem. Concr. Res. 34 (2004) 1683–1696.
[67] T. Ichikawa, Alkali– silica reaction, pessimum effects and pozzolanic effect, Cem. Concr. Res. 39 (2009) 716–726.